Investigation of the Molecular Motion of Self-Assembled Fatty Acid Films

T. Risse,* T. Hill, J. Schmidt, G. Abend, H. Hamann, and H.-J. Freund

Fritz-Haber Institut der Max-Planck-Gesellschaft, Faradayweg 4-6, 14195 Berlin, Germany

Received: July 28, 1997; In Final Form: November 25, 1997

We have investigated self-assembled stearic acid films adsorbed on an Al_2O_3 film by means of electron paramagnetic resonance (EPR) as well as near-edge X-ray absorption fine structure (NEXAFS) spectroscopy. The stearic acid molecules are orientated in the film as shown by the NEXAFS data. Doping of the film with spin-labels in order to make the films accessible to EPR spectroscopy distorts the structure only slightly as long as the concentration of the spin-labels is low. The temperature-dependent EPR spectra reveal a distinct dependence of the onset of the rotational motion of the spin-label with variation of the location of the spin-label along the chain. The analysis of the EPR line shape allows to gain insight into the internal motion of the molecular chain.

1. Introduction

Self-assembled monolayers as well as Langmuir−Blodgett films have attracted considerable interest over the past years.[1] Especially in connection with technological applications, e.g., highly specific sensors or devices based on molecular electronics, these structures may play a role in the future.[2,3] Ultrathin organic structures have been investigated in the past by several experimental as well as theoretical methods. However, experimental investigations of dynamic properties, especially of internal molecular dynamics of these films, are rare. EPR spectroscopy can provide insight into the rotational motion of molecules on surfaces. In contrast to NMR, an important tool for the investigation of molecular motion in liquid and solid phases,[4] EPR spectroscopy can provide information about molecular motion on solid single-crystal surfaces in submonolayer coverage[5,6] due to the extremely high sensitivity of the method (10^{12} spins) in comparison with NMR spectroscopy (10^{17} spins). A disadvantage of the EPR method is the necessity of an unpaired electron to obtain an EPR signal. However, if the molecule carries an unpaired electron, the analysis of the anisotropic magnetic structure of radical centers can give useful information about dynamics, orientation, concentration, or chemical environment of the species.

In this study we want to present a combined EPR and NEXAFS spectroscopic investigation of self-assembled fatty acid films. Part of the EPR data have been published in a short version before.[7] It is known from the literature that fatty acids form self-assembled monolayers on oxide surfaces.[8,9] We have adsorbed the organic monolayer on a thin Al_2O_3 film in order to be able to perform the EPR as well as the NEXAFS experiments on the same, well-defined substrate. It is well-known that the order of the self-assembled monolayers increases with increasing chain length; therefore, we have used stearic acid ($C_{18}H_{36}O_2$) as a model substance here. Introducing paramagnetic spin-labels into the structure, these films become suitable for EPR spectroscopy. We have used *n*-doxyl stearic acid (*n*-DXSA) where the paramagnetic group, an oxazolidinyl ring, is connected to different positions of the hydrocarbon chain. These spin-labels are well-known as paramagnetic probes for example in the study of natural and synthetic membranes.[10]

2. Experimental Section

The EPR measurements were performed in a specially designed ultrahigh-vacuum chamber which has been described in detail elsewhere.[11] The electronic part of the EPR spectrometer (Bruker B-ER 420) has been improved by a new X-band microwave bridge (Bruker ECS 041 XK) and a lock-in amplifier (Bruker ER 023 M). This modification led to a considerable increase in the signal-to-noise ratio. The ultrahigh-vacuum chamber was equipped with a quadruple mass spectrometer as well as a combined LEED/Auger unit in order to characterize the substrate.

The NEXAFS spectra were recorded at the storage ring BESSY (Berliner Elektronenspeicherring-Gesellschaft für Synchrotronstrahlung mbH, Berlin) using the HETGM2 monochromator. The ultrahigh-vacuum chamber has been described previously.[12] The spectra were recorded in partial yield mode with a retarding voltage of −120 V. The experimental resolution was approximately 1 eV at the C 1s edge. The raw spectra were normalized to the incident photon flux by dividing through a spectrum of the clean, freshly prepared Al_2O_3 film. The energy calibration was done by measuring the Al 2p signal of the substrate with light of first and second order.

The Al_2O_3 film was prepared on a NiAl(110) single crystal (cut to within <0.5%) according to the recipe by Jaeger et al.[13] After cleaning the substrate (cycles of sputtering with Ar ions and annealing to 1000 °C), the crystal was oxidized, and afterward the crystal was annealed to develop a thin, well-ordered, dense Al_2O_3 film.

The doxyl stearic acids as well as the pure stearic acid were purchased (Sigma, Munich) and used without further purification. The fatty acid films were prepared by immersion of the Al_2O_3 substrate into a mixture of *n*-doxyl stearic acid and stearic acid in toluene. The overall concentration of the molecules in the solution was always 1 mM. The molar fraction of each component is given for each experiment in the text. The temperature of the solution was room temperature in the case of the 5-doxyl stearic acid films and 28 °C in the case of the 12- and 16-doxyl stearic acid films. This difference is due to the fact that the adsorption behavior depends considerably on temperature of the solution in the case of the 12- and 16-doxyl stearic acid.[14] The immersion times were varied between 24

S1089-5647(97)02459-0 CCC: $15.00
Published on Web 03/17/1998

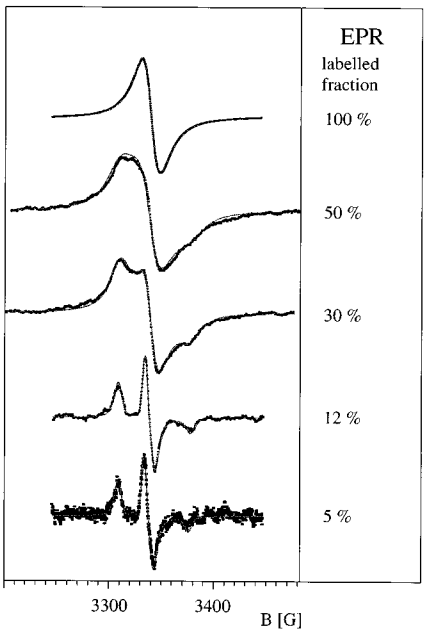

Figure 1. Concentration-dependent EPR spectra of 5-doxyl stearic acid films at room temperature. Spectra are normalized to constant peak-to-peak height. Dots indicate the measured spectra; the full lines represent computer simulations.

and 100 h without any effect on the resulting spectra. After being removed, the sample was rinsed several times with toluene and subsequently with ethanol and water. The crystal was dried in air and afterward transferred into the vacuum chamber. During the EPR measurements the pressure of the chamber was lower than 10^{-7} mbar. Under these conditions the self-assembled films were stable for weeks.

The program used to simulate the line shape of the EPR spectra was basically written by Beckendorf.[15] The description of the molecular motion is based on a program package developed by Freed and co-workers,[16] which utilizes the solution of the stochastic Liouville equation for the description of dynamic processes.[17]

3. Results and Discussion

3.1. Concentration Dependence of the EPR Spectra. For the discussion of dynamic effects in the following sections, it is important to make sure that intermolecular spin−spin interactions which may obscure the determination of the **g**- and **A**-tensor components of the spin-labels in the rigid limit are unimportant for the measured spectra, since a meaningful analysis of the dynamic effects crucially depends on correct **g**- and **A**-tensor components.

Figure 1 shows the EPR spectra of 5-doxyl stearic acid films for different fractions of labeled molecules in the film. The amounts of labeled molecules given in Figure 1 refer to the molar fraction of those molecules in solution. To determine the fraction of labeled molecules on the surface, it is necessary to ascertain the amount of labeled as well as the amount of unlabeled molecules on the surface. The number of labeled molecules can be evaluated at least relatively by means of the EPR intensities whereas the quantity of unlabeled molecules is difficult to obtain. However, as an estimation for the concentration of the labeled molecules it is worthwhile looking at the EPR intensities. In Figure 2 we plot the intensities determined from the spectra presented in Figure 1 versus the fraction of the labeled molecules in the corresponding film. To visualize the changes more clearly, the intensities are plotted on a

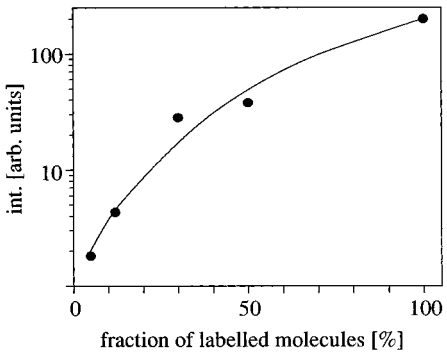

Figure 2. Intensities of the concentration-dependent spectra of Figure 1.

logarithmic scale. The intensities decrease very rapidly with decreasing fraction of labeled molecules. The intensity drops by a factor of 100 going from the prepared exclusively pure labeled molecules to the highly diluted film (5%).

This phenomenon can be understood on the basis of the energetics of the adsorption process. The energy balance of the adsorption process is mainly determined by two large contributions. First the strong interaction of the headgroups with the substrate and second the van der Waals interaction between the long alkyl chains have to be taken into account. Consider that at the very beginning of the adsorption process the coadsorption of two different (labeled and unlabeled) molecules will be random. Consequently, the proportion of labeled molecules on the surface will be equal to that in the solution. Therefore, the EPR intensity should decrease almost linearly with the concentration of the labeled molecules. The discrepancy between this prediction for the very beginning of the adsorption process and the intensities measured and plotted in Figure 2 could be explained by taking the ordering process which lasts on the order of several hours into account. During this period labeled molecules will be removed from the film, due to the steric demand of the spin-labels. The removal will simultaneously increase the number of molecules as well as the number of van der Waals contacts in the film and thus minimize the total energy of the film. A similar phenomenon was found by Offord et al. while coadsorbing *n*-alkanethiol as well as terminal *tert*-butanethiol on a gold surface.[18] The probability of finding the terminal *tert*-butanethiol in the self-assembled film was dramatically decreased compared with the *n*-alkanethiol. As pointed out above, the decrease of intensity to 1% in the film prepared from a solution containing 5% labeled molecules is insufficient to conclude that the film really contains 1% of labeled molecules. Nevertheless, referring to the discussion of the steric demand of the spin-label, it should hold as an upper limit for the concentration of the labeled molecules on the surface.

The change in the line shape with decreasing concentration of the labeled molecules can easily be recognized and will be considered next. The spectrum of the pure labeled film, shown at the top of Figure 1, reveals a single almost Lorentzian line with a peak-to-peak width of 19 G (33 G fwhm), whereas the spectra at 12% and 5% labeled molecules show a well-resolved spectrum due to **g**- and **A**-tensor anisotropies with a line width of 7.9 and 7.5 G (fwhm), respectively. The spectra taken at an intermediate molar fraction in the solution show an increase in the line width with respect to the pure labeled film, but only marginal evidence for magnetic anisotropies expected for the spin-label for the 50% solution. However, the spectrum at 30% molar fraction clearly reveals indications for the ^{15}N hyperfine interaction of the spin-label. Nevertheless, the line width is

TABLE 1: Summary of the Parameters Used To Simulate the Spectra from Figure 1

fraction, %	ν_{ex} [Hz]	intensity [arb units]	$\Delta B_{1/2}$ [G]
100	$\sim 8 \times 10^{10}$	1.9×10^6	33
50	7.2×10^7	3.7×10^5	29
30	2.7×10^7	2.8×10^5	23
12		4.3×10^4	7.9
5		1.8×10^4	7.6

TABLE 2: Parameters Used To Fit the NEXAFS Spectra of Stearic Acid as Well as 16-Doxyl Stearic Acid Films

	step	R*	CC*	CC′*
postion [eV]	288.6	288.2	293.4	301.5
width [eV]	1.9	1.4	2.6	5.3
slope [eV^{-1}]	−0.0014			

TABLE 3: g- and A-Tensor Components for the Different *n*-Doxyl Stearic Acids

	g_x	g_y	g_z	A_{xx} [G]	A_{yy} [G]	A_{zz} [G]
from ref 59	2.0088	2.0061	2.0027	6.3	5.8	33.6
5-DXSA	2.0089	2.0062	2.0027	6.4	5.9	33.5
12-DXSA	2.0089	2.0063	2.0027	6.1	5.6	32.7
16-DXSA	2.0088	2.0059	2.0027	6.0	5.7	33.8

plainly increased compared with the spectra at low concentrations. The collapse of the anisotropies in the EPR spectra observed for the highly concentrated films is due to exchange interactions of the spin-labels. Because of the strong distance dependence of the exchange interaction, the line width of the pure labeled film provides evidence for the density of the molecules in the film. Comparing the line width of the pure labeled film (19 G ΔB_{pp}) with the line width of the pure 5-doxyl stearic acid powder as provided by Sigma (18 G ΔB_{pp}), it can be concluded that the intermolecular distance between two spin-labels is comparable in the two systems. Bonosi et al.[19,20] have investigated Langmuir−Blodgett films on a stearic acid precovered quartz substrate and measured a line width of 24 G (peak-to-peak) for 5-doxyl stearic acid films. The larger line width of these systems compared with the self-assembled film is indicative of an increased intermolecular distance of the spin-labels in these systems.

To quantify the variation of the exchange interaction within the concentration series, we perform simulations on the basis of the Liouville approach shown in Figure 1 as full lines. The parameters used to simulate the spectra are shown in Tables 1 and 3. The qualitative statement that the topmost spectrum is dominated by exchange effects which decrease with decreasing fraction of labeled molecules is confirmed by the simulation. For the topmost spectrum the simulation results in an exchange frequency of 8×10^{10} Hz. Although the Liouville approach used here describes the exchange only approximately,[16] and the precise value of the exchange frequency determined thereby maybe incorrect, the trend toward the other spectra with lower concentrations of labeled molecules is clearly visible. As can be seen in Table 1, the exchange frequency decreases rapidly with decreasing concentration of labeled molecules. The two films with lowest concentration do not show any exchange effect at all. This is due to the fact that exchange frequencies lower than approximately 10^7 Hz affect only the line width rather than the shape of the spectrum. However, the line width is an independent parameter in the simulations; therefore, one cannot easily distinguish between the exchange effects and other effects that cause homogeneous line broadening once the exchange frequencies are small. It is worthwhile to mention that the decrease of the line width is much less rapid than the decrease of the exchange effects. While the exchange interaction has almost vanished at a concentration of 30% labeled molecules, the line width drops until the concentration of labeled molecules is below approximately 10%. This is consistent with the fact that the line width is determined not only by the short-range exchange interaction but also by other long-range interactions as for example dipolar interactions of the spin-labels. To verify that the spectra at low concentration are representative for magnetically independent spin-labels, we compare the line widths of these films with the line widths of highly diluted frozen solutions of the molecules. We find very similar results for the films and for the diluted solutions. Because intermolecular interactions of the spin-labels are attenuated in highly diluted solutions, one may conclude that the molecules in the films with low concentration of the spin-labels are magnetically independent.

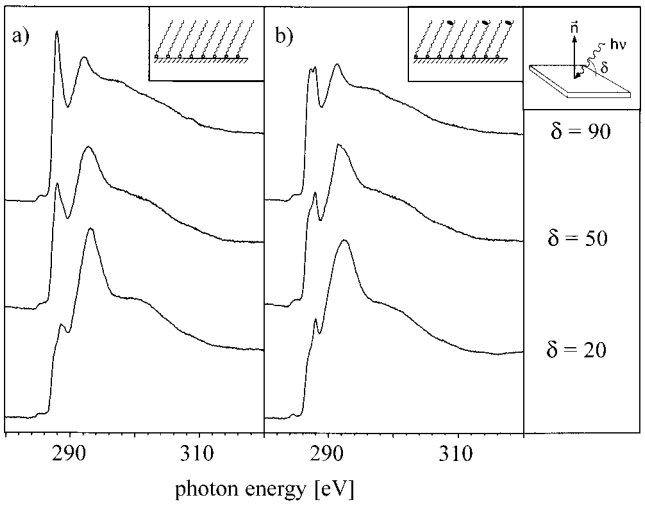

Figure 3. NEXAFS spectra of self-assembled (a) stearic acid film and (b) 3% 16-DXSA film on Al_2O_3/NiAl(110). Spectra are normalized to constant edge jump. δ is the angle between the surface and the direction of the incident light.

3.2. NEXAFS Spectroscopy. Figure 3 shows the X-ray absorption spectra of a pure stearic acid film (left panel) and a stearic acid film doped with 3% 16-doxyl stearic acid (right panel) at different photon incident angles recorded at the C 1s adsorption edge. The fine structure of the adsorption signal in the vicinity of the C 1s edge is due to excitations into unoccupied molecular orbitals of the hydrocarbon chain. The spectra of hydrocarbon chains are dominated by two resonances. The first resonance below the adsorption edge at 288 eV has been interpreted as being an excitation into a molecular orbital of predominately C−H antibonding character.[21,22] More recently, Bagus et al. have shown that these resonances can be attributed to a superposition of several Rydberg orbitals.[23] The second resonance occurs at 293 eV and is interpreted as an excitation into a CC antibonding orbital. In addition, the spectra reveal a third resonance at 301 eV which is less intense and has been attributed to be of CC antibonding character because of its angular behavior.

The intensities of the NEXAFS resonances show a strong variation with the angle of photon incidence, as can be seen in Figure 3. The change in the intensities is different in sign for the Rydberg resonance (R*) and for the two resonances of CC antibonding character. This large linear dichroism documents a high degree of molecular orientation of the molecules in the alkyl chain. The variation of the resonance intensities can be used to determine the orientation of the molecules. The angular dependent intensities are determined by a fitting scheme that has been initially proposed by Outka et al.[22,24] To obtain

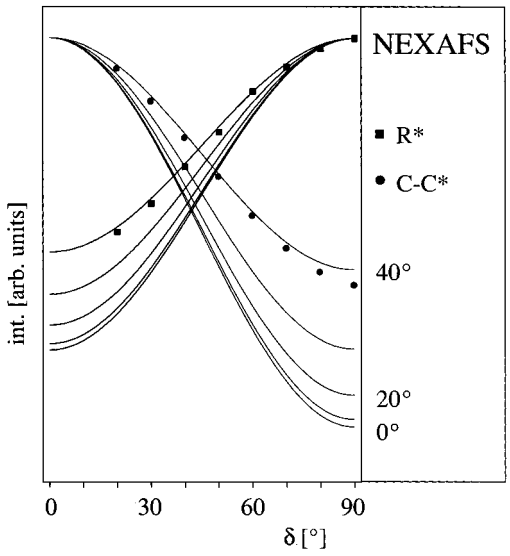

Figure 4. Angular variation of the NEXAFS Rydberg and CC resonance intensities according to the analysis scheme for the pure stearic acid film. δ is the angle between the surface and the direction of the incident light.

reasonable results, this scheme has been modified later by Hähner et al.[25] However, a deconvolution of the spectral features is difficult due to the narrow spacing of the structures as compared to the limited resolution. Therefore, a different method based on numerical integration of difference spectra has been proposed in the literature.[26] The drawback of this method is the necessity of reference systems with known orientation of the molecules in order to determine the unknown excitation probability S_Ψ from the C 1s into the given molecular orbital Ψ.[26,27]

Apart from the three resonances already mentioned, the spectra exhibit a small resonance structure below the Rydberg resonance at 285−286 eV. This structure has been found previously by several authors. It has initially been attributed to an insufficient correction of the monochromator characteristic.[22,28] Further experiments have shown that this structure may be related to radiation damages of the system,[29,30] e.g., the formation of C═C double bonds. For the present results we cannot rule out both explanations; however, one might expect that the intensity of this structure should gain intensity with increasing exposure to the soft X-ray photons if the structure is related to radiation damages. The spectra do not exhibit any significant change during the measurements. Nevertheless, a contamination of the film with C═C double bonds, e.g., with toluene molecules from the solution, may explain this additional resonance.

A comparison of the spectra recorded for the two systems reveals that the strong linear dichroism caused by the high degree of molecular orientation decreases through the doping of the film with spin-labeled molecules. Especially the features of the Rydberg resonances are effected whereas the angular variation of the CC resonance remains almost constant. Comparable effects were found for incompletely ordered docosanethiol films[27] or temperature-induced disorder in LB as well as in self-assembled films.[31]

Figure 4 shows the intensity variation of the Rydberg and the CC antibonding resonance together with the theoretically predicted angular behavior of the intensities. The determination of the intensities was performed according to the fitting scheme proposed by Outka et al.[24] Within this scheme the absorption edge was described by an error function. The positions of the signals were determined from difference spectra, and the intensities were achieved by fitting Gaussian functions to the spectra. The parameters used to fit the spectra are shown in Table 2.

The calculation of the angular variation for an assumed geometry requires information about the orientation of the transition dipole moments (TDM) for the different resonances relative to the molecular framework. The orientation of the TDM can be deduced by means of group theoretical arguments as long as the symmetry of the molecule is high.[32] For molecules with reduced symmetry exact quantum chemical calculations including the core hole are required. Owing to the complexity of the theoretical problem, the so-called "building-block" scheme has been used to determine the orientation of the TDM. However, Hähner et al. have shown that the building-block scheme is insufficient for the description of the TDM in long hydrocarbon chains.[25] The curves shown here are calculated according to the orientation used by Hähner et al., namely, a TDM oriented parallel to the long axis of the molecule for the CC resonance and perpendicular to that direction for the Rydberg resonance. The same orientation of the TDM would be expected by group theoretical considerations assuming an all-trans conformation of the alkyl chains.[33] In the case of the Rydberg resonance, theoretical[34] as well as experimental investigations[35] show that this resonance consists of two different peaks which are separated by ∼0.5 eV. Accordingly, the simulation includes the presence of two components with an intensity ratio of 0.7.

A comparison of the theoretical curves with the experimental data indicates that good agreement is obtained for a tilt angle of 37°. Comparing this result to the tilt angle of 10° found by Allara and Nuzzo for a fatty acid film adsorbed on an Al_2O_3 substrate, the value of 37° is rather high.[8,9] However, there are several aspects that should be taken into account when comparing these values. The adsorption geometry of the molecules in a self-assembled film depends rather strongly on the density of adsorption sites on the surface. Whereas long-chain alkyltrichlorosilane builds up films with molecules oriented perpendicular to the surface,[29] alkanethiols on gold form a structure where the molecules are tilted by 35°.[36] The explanation for this behavior is that due to the increased distance between the headgroups, the molecules have to be tilted in order to give an equivalent spacing between the alkyl chains. As the structure of the well-ordered Al_2O_3 film used here may deviate significantly from the amorphous substrates used in the other experiments, this distinction may partly account for the variation of the observed tilt angle. Furthermore, one should note that there are also considerable differences within the results reported in the literature so far.[37−39] The difference between the groups are mostly attributed to unlike preparation procedures, e.g., substrates, concentration of the molecules, or temperature of the solution. Finally, it is worthwhile to mention that with NEXAFS spectroscopy one may determine only the average tilt angle, so that the signal may result from a superposition of patches where the molecules are in more upright positions and areas with higher degree of disorder.

The right panel in Figure 3 shows NEXAFS spectra of a 16-doxyl stearic acid film. As it was pointed out earlier, the line shape of the spectra, especially the structure of the Rydberg resonance, changes considerably, whereas the shape of the CC resonance above the absorption edge remains almost constant. In contrast to the spectra of the pure stearic acid film, the Rydberg resonance now consists of two clearly separated structures. In analogy to the pure stearic acid film, the

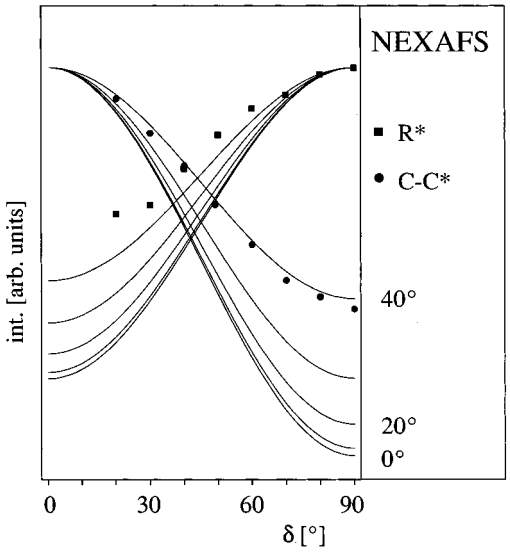

Figure 5. Angular variation of the NEXAFS Rydberg and CC resonance intensities according to the analysis scheme for a 16-doxyl stearic acid film. δ is the angle between the surface and the direction of the incident light.

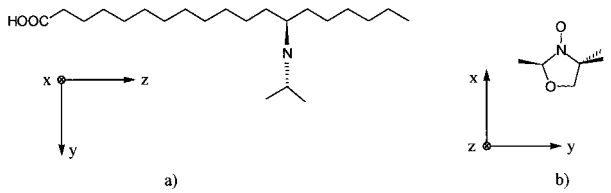

Figure 6. Schematic representation of a 12-doxyl stearic acid molecule in all-trans conformation: (a) side view, (b) top view. The chain in part b continued in the *z*-direction connected to the carbon atom between the two heteroatoms of the ring.

determination of the angular dependent intensities was repeated. Within the fitting scheme of Outka et al.,[24] the position and the slope of the adsorption edge were treated as parameters in order to get a consistent description of the tilt angle for Rydberg as well as for the CC resonance. Since both systems, namely the labeled and the unlabeled film, are almost identical, we used the same parameters for the CC resonance and the adsorption edge, whereas the positions of the Rydberg resonances were readjusted to describe the intensity in this region properly. The analysis of the angular dependent intensities led to inconsistent results, as can be seen in Figure 5. The analysis of the Rydberg resonance predicts a tilt angle of 45° whereas the analysis of CC resonance leads to a tilt angle of 38°. The failure of the method is directly connected to the difference in the changes of the two resonances. Schertel et al. report on similar changes in the NEXFAS spectra of LB as well as self-assembled thiol films due to thermally induced gauche defects.[27] The authors ascribe the changes in the NEXAFS spectra to a change in the electronic structure of the film. Considering the fact that the resonance has dominantly Rydberg character, which implies that the unoccupied orbitals are fairly large, it is reasonable that this resonance is very sensitive to conformational changes of the chain. Then the change in the NEXAFS spectra could be caused by the formation of gauche conformations in the structure. To see this, we consider the "ideal" structure of the doxyl stearic acid. Figure 6 shows a top as well as a side view of a 12-doxyl stearic acid molecule in the trans conformation. It is easy to rationalize from the top view that the adsorption of trans conformed molecules around such a spin-labeled molecule would lead to free space in the area below and above the

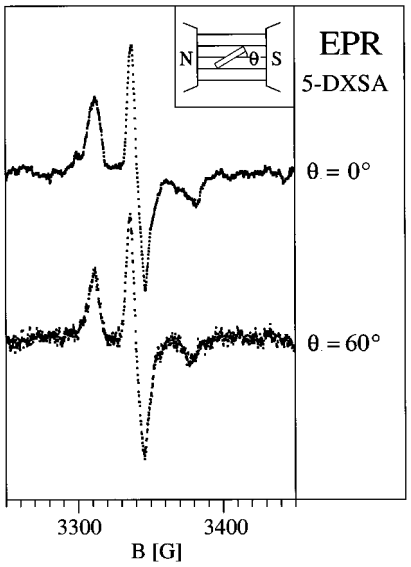

Figure 7. Angular dependent EPR spectra for a 5-doxyl stearic acid film.

spin-label. Such a situation is not stable and will be stabilized by minimizing the spatial distortion of the structure in order to maximize the number of van der Waals contacts within the film. This can be achieved by introducing gauche conformations so that the spin-label will be tilted toward the long axis of the molecule. But this distortion will not be restricted to spin-labeled molecules and will also affect the surroundings. Therefore, one would expect that the amount of trans conformation, and thus well-oriented molecules, in the structure will decrease as the concentration of the spin-label increases. The investigation of 15% and 50% 16-doxyl stearic acid films corroborates this prediction. Whereas the 15% films exhibit very small angular dependencies of the NEXAFS spectra, the spectra of the equimolar film show no angular dependency at all.

3.3. Angular Dependence of the EPR Signal. Assuming an ideal structure of the self-assembled film as depicted for example in the insets of Figure 3, the molecules would all be in the trans conformation. The plane of the heterocyclic ring of the spin-label would be oriented perpendicular to the backbone of the hydrocarbon chain as shown in Figure 6. The EPR spectra of such a ensemble would exhibit a strong dependence on the angle between the static magnetic field and the surface. Behavior like this is often found for single crystals so that the different components of the **g**- and **A**-tensors could be determined independently.[40]

Figure 7 shows the spectra of a 5-doxyl stearic acid film for two selected angles between the static magnetic field and the surface. As can be seen, the spectra reveal almost no angular dependence at all. Therefore, we conclude that the anisotropy of the spin-label orientation is very low. That seems to contradict the experimental results presented so far. However, one should bear in mind that the **g**- and **A**-tensors of the spin-label used here are almost axial symmetric. This implies that the *z*-axis (see Table 3 and Figure 8) of the molecule has to be involved in the anisotropic distribution of the molecules in order to result in angular dependent EPR spectra. It is clear from the discussion of the NEXAFS spectra in the last section that the picture of the ideal structure assumed to predict the angular dependency cannot be maintained. Apart from a tilt of the molecules with respect to the surface normal, the doping of the film with the spin-labels induces a considerable amount of gauche defects. In the case of a chain in a trans conformation

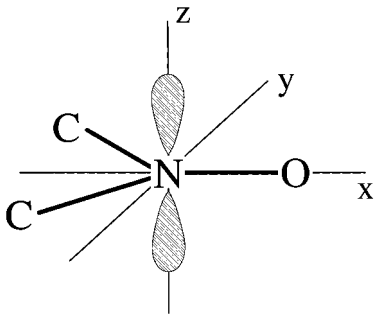

Figure 8. Principal axis of the **g**- and **A**-tensors for the nitroxides.

the rotation of the molecule should be hindered due to the rigid connection between the headgroup and the substrate. This rigid orientation of the spin-label relative to the long molecular axis is, however, lifted owing to the introduction of gauche defects. Consequently, quantities such as the twist angle (angle between the plane defined by the surface normal and the long axis of the molecule and the plane of the carbon atoms in the hydrocarbon chain) determined experimentally to 55° for thiols on gold[41,42] are not defined any longer. The introduction of gauche conformations will optimize the structure of the film with regard to the packing of the molecules. Because of the large number of degrees of freedom, more than one orientation with similar energetic should be possible so that the equilibrium structure is characterized by a variety of orientations of the spin-label with respect to the framework of the static magnetic field. On the other hand, the number of orientations necessary to mimic an isotropic distribution is rather low as long as the line width is of the order of 8 G. Katter[43] has shown that the assumption of 10 orientations distributed statistically about the azimuth and seven about the polar angle are sufficient to simulate an isotropic spectrum. According to the preceding discussion, it should be easy to fulfill this requirement in the present case.

3.4. The Regime of Rigid Spin-Labels. *3.4.1. 5-Doxyl Stearic Acid Films.* Figure 9 presents the EPR spectra of a 5-doxyl stearic acid film with a concentration of 8% in the temperature range between 60 and 300 K. We would like to note at the beginning that the overall intensity of the spectra behaves according to Curie's law. The line shape of the spectra shows only minor changes; in particular, no further structures occur in the spectra as would be expected for rotationally excited molecules. However, with decreasing temperature the line width of the spectra increases as can easily be verified for the minimum at around 3320 G. The spectrum at 300 K shows an approximately 15 G wide plateau with virtually no intensity in this region. While decreasing the temperature this plateau shrinks to a V-like shape, and finally one finds intensity in the whole region due to the broadening of the lines. To quantify this observation, it is necessary to simulate the line shape of the spectra.

The simulation of the line shape requires the knowledge of the molecular constants, namely the **g**- and **A**-tensors. The exact values of the tensor components depend on the environment of the molecules. Therefore, it is necessary to determine these constants for the investigated systems. It is crucial to perform the determination of the constants for rigid molecules because the rotational motion of the molecules on the time scale of the experiment would tend to lower the anisotropy of the tensor. A notable way to determine the values is to measure at the lowest possible temperature because this ensures the required rigidity of the molecules best. We note, however, that the determination

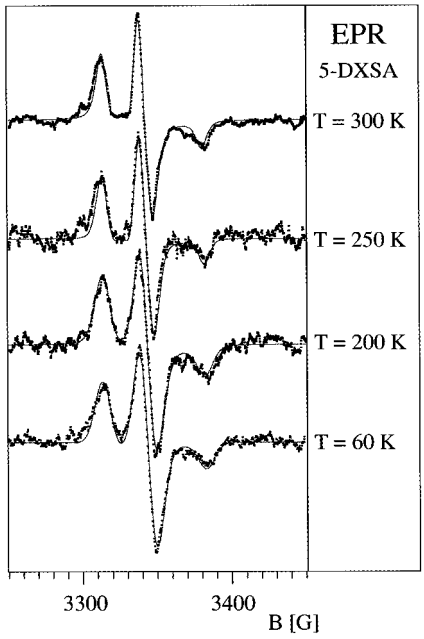

Figure 9. Temperature-dependent EPR spectra of a 5-doxyl stearic acid film between 60 and 300 K. Points represent the measured spectra and full lines the corresponding simulations. The spectra are normalized to a constant peak-to-peak-height.

of the constants would be more precise for spectra with narrow lines, namely the spectra at room temperature.

Another important piece of information for the calculation of the rigid limit spectra is the knowledge of the spatial distribution of the molecules. As the spectra do not exhibit any angular dependencies, we use a statistical, three-dimensional ensemble of molecules to simulate the spectra. The line shape was chosen to be Lorentzian following the results of prior investigations,[6,44] and the starting values of the **g**- and **A**-tensor components were taken from the literature (see Table 3). To get a satisfactory fit, it was necessary to change the *x*- and *y*-components of the **g**-tensor considerably. This is an unusual behavior as most experimental investigations report quite similar values for spin-labels in hydrophobic surroundings.[45−48] Furthermore, the simulation of the temperature-dependent spectra carried out with these molecular constants does not lead to a satisfactory fit. Trying to simulate the spectra with tensors adjusted to another spectrum of the series failed as well. This failure is caused by the fact that not only the line width but also the line shapes of the spectra change with decreasing temperature. Therefore, we choose a so-called Voigt profile (the convolution of a Gaussian and a Lorentzian profile) in order to describe homogeneous as well as possible inhomogeneous line broadening. The results for the simulation of the spectra are shown as full lines in Figure 9, and the corresponding parameters are plotted in Figure 10. The upper chart presents the Gaussian fraction separately whereas the lower one shows the corresponding line width (fwhm) for two different film preparations. Both quantities show almost the same temperature behavior. At low temperatures up to approximately 120 K the spectra exhibit pure Gaussian lines. The Gaussian fraction decreases to about 30 % while increasing the temperature to 230 K. The line width lowers simultaneously from 11 G in the low-temperature regime to 8 G above 230 K. In the temperature range between 120 and 230 K the behavior is not uniform. Whereas the Gaussian fraction has decreased to 70% at 166 K the line width is still 11 G. However, the simulation for the spectrum at 200 K reveals a constant Gaussian fraction

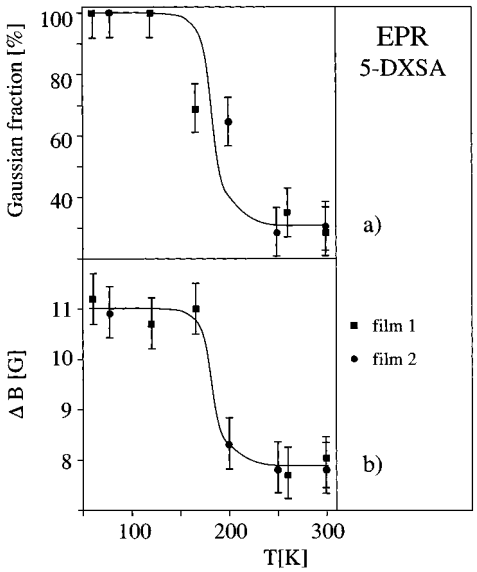

Figure 10. Temperature dependence of the Gaussian fraction (a) and the line width (b) shown for two 5-doxyl stearic acid films. Rectangles and circles represents two different preparations.

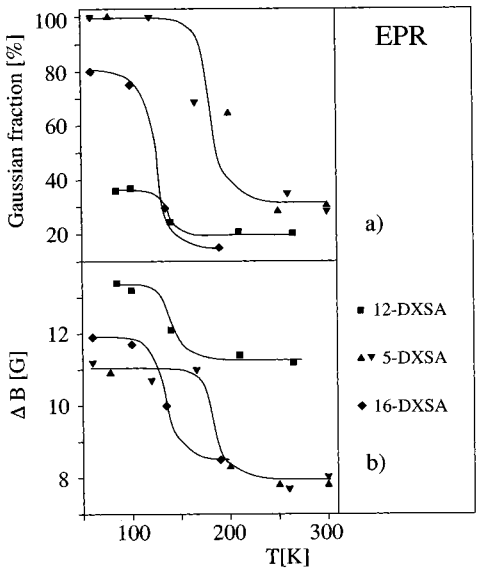

Figure 11. Temperature dependence of the Gaussian fraction (a) and the line width (b) compiled for 5-, 12-, and 16-doxyl stearic acid films. The different triangles represent two different preparations of the 5-doxyl stearic acid film.

with a line width of 8.3 G. It is worthwhile to note that these two spectra belong to two different preparations with slightly different concentrations of the labeled molecules in the solution, namely 10% and 8%, respectively.

A quantification of the error bars for the two quantities is difficult. Since the result of the fit is influenced by the choice of the starting parameters, the error bars shown here are mean variations for a variety of simulations with different starting parameters and almost equivalent results.

3.4.2. 16-Doxyl Stearic Acid Films. Comparing the spectra of the 5-doxyl stearic acid film with a 16-doxyl stearic acid film, the principal behavior of the 16-doxyl stearic acid film in the rigid limit regime is not different from that of the 5-doxyl stearic film. The line widths as well as the Gaussian fractions of the line shapes increase with decreasing temperature. However, the temperature range for the molecules to be rigid on the time scale of the experiment is considerably lower than in the case of the 5-doxyl stearic acid films. For temperatures above 190 K the spectra of the 16-doxyl stearic acid film exhibit dynamical effects of the spin-label. Due to the low-temperature range, the number of measurements is relatively low so that the line through the data points in Figure 11 should be understood in analogy to the behavior of the 5-doxyl stearic acid film. According to Figure 11, even a linear increase of the line width and the Gaussian fraction would fit to the data points.

3.4.3. 12-Doxyl Stearic Acid Films. In the case of the 12-doxyl stearic acid film, one should expect a behavior intermediate between the two cases already discussed. However, the simulations of the 12-doxyl stearic acid films reveal a significant difference compared to the other systems as can be seen in Figure 11. In this case the change of the Gaussian fraction of the line shape is rather small. The line width increases by 2.2 G compared to 3 G for the other systems. It should be noted that the initial line width at higher temperatures is 11 G compared to 8 G in the case of 5- and 16-doxyl stearic acid. This increase in line width is due to the fact that the molar fraction of the solution was 15% compared to 8−10% for 5- and 16-doxyl stearic acid films. The spectrum of a film doped with 8% 12-doxyl stearic acid reveals a line width of 8.5 G, in accord to the values found for 5- and 16-doxyl stearic acid.

Because of the large initial line width, it no longer justified to assume an anisotropy of the *x*- and *y*-components of the **g**- and **A**-tensors to fit the spectra. These spectra can be simulated assuming axial symmetric **g**- and **A**-tensors in analogy to experiments for DTBN on Al_2O_3 by Katter et al.[44] Moreover, the spectra could satisfactorily be simulated by assuming a simple Lorentzian line shape rather than a Voigt profile without significant changes in the values of the tensors. However, the spectrum for the diluted system with a line width of 8.5 G is simulated best with tensors similar to those used to describe the other systems.

3.4.4. Discussion of the Experimental Results. The behavior of the three systems can be summarized as follows: (i) The onset temperature for the molecular motion of the spin-label on the time scale of the experiment decreases considerably while shifting the spin-label along the alkyl chain toward the surface. (ii) The line shape of the spectra could be described by a Voigt profile. (iii) The line width as well as the Gaussian fraction of the Voigt profile increases with decreasing temperature. The extent of the effect differs from system to system. The Gaussian broadening of the spectra can be explained by all effects that cause inhomogeneous broadening of lines, e.g., inhomogeneities of the magnetic field. Experimental reasons can be ruled out in this case as the experimental conditions were constant for all measurements presented here. We therefore look for an alternative explanation.

An effect that causes inhomogeneous line broadening of EPR signals is unresolved hyperfine interactions. EPR as well as ENDOR measurements of doxyl-substituted cycloalkanes show that the hyperfine interaction of the spin-label to protons of the alkyl chain could be quite large.[49−51] The temperature-dependent ENDOR experiments by Eaton et al. reveal a hyperfine interaction of 2 G between the spin-label and the protons bound to the α C atom when the isomerization of the ring inversions is very slow on the time scale of the EPR experiment. In the case of fast isomerization the authors report on four equivalent protons with an hyperfine splitting of only 0.4 G.[51−53] Moreover, the coupling to the protons bound to the β C atom are approximately 0.5 G in the rigid limit case. The hyperfine interaction of the spin-label to the protons of both methyl groups is, however, rather weak, namely 0.1 G.[49] This

is probably due to the fact that the rotational motion of the methyl groups is fast. For solutions of noncyclic hydrocarbons, one would not expect strong hyperfine splittings as the rotation around the C−C bond is always fast on the time scale of the experiments. However, for densely packed hydrocarbon chains, as investigated here, the rotation of the C−C bound can be frustrated due to a lack of free space. Considering for example a trans−gauche isomerization of a single C−C bond remaining, the rest of the chain fixed would lead to a bend in the chain. According to the enormous steric demand, these motions are very unlikely for densely packed molecules. However, several kinds of motions are discussed in the literature in order to overcome the steric problem, e.g., the so-called "crankshaft" mode.[54] All of these models are based on the assumption that two such trans−gauche isomerizations occur close in space and time. Nevertheless, those motions are only possible if there is enough unoccupied space in the structure. This discussion shows that the motion of molecules or molecular segments in densely packed systems cannot be described in terms of the local mobility of a single molecule. In fact, the mobility of the whole system has to taken into account as the possibility for the motion of a single molecular segment is determined by the dynamics of all neighbors. Further problems related to the description of motions in densely packed systems are discussed in the literature.[55−57]

Considering this discussion, we propose that the Gaussian broadening of the EPR spectra is caused by the rotational motion of the methylene groups connected to the spin-label. Chidsey et al. report on the loss of the diffraction peaks in a helium atom scattering experiment of a thiol film on gold at temperatures above 100 K.[58] The authors attribute this effect to the motion of the terminal alkyl groups of the film. Comparing this observation to the onset of the protons motion for the 16-doxyl stearic acid film of approximately 130−140 K, one finds a good agreement between the two experimental results. The hyperfine splitting of the lines should be comparable for the three systems assuming similar motions of the methylene groups in all cases. The observed line shapes and widths are due to the convolution of the homogeneous line width with the spectral distribution function. Therefore, the effect due to a constant broadening of the spectral distribution function for the different systems would lead to a less pronounced effect for higher initial line width. Furthermore, the increase of the line width in the case of the 12-doxyl stearic acid film is only 2.2 G compared to 3 G for the other systems; this may indicate that the density of the film decreases when the concentration of the spin-labels increases. Due to the decrease of the density of the molecules, the space necessary for the motion of the molecules would increase. Consequently, one has to cool the system to lower temperatures in order to freeze the rotational motion. Therefore, the spectrum of the 12-doxyl stearic acid film may not represent the rigid limit of the methylene rotation. Further changes in the motional behavior for the spin-label of the film that corroborate the interpretation given above are found at higher temperatures and will be discussed separately.[14] These findings indicate that it is necessary to prepare films with sufficiently low concentration of spin-label not only to avoid intermolecular spin−spin interaction but also to probe the dynamics of densely packed systems, because the decrease of the films density changes the dynamic behavior of the film drastically. Below a certain concentration of the spin-label, namely 10%, any changes in the dynamic behavior occur; however, these film exhibit the same dynamic behavior as films with high spin-label concentration after disruption of the film structure due to a thermal treatment. This result corroborates the assumption that the EPR spectroscopy of highly diluted films probes the dynamics of densely packed films.

4. Summary and Conclusion

In summary, we have shown concentration- and temperature-dependent EPR as well as NEXAFS spectra of self-assembled stearic acid films containing different *n*-doxyl stearic acids as spin probes. According to the concentration-dependent investigations, it is possible to prepare self-assembled monolayers with magnetically almost independent spin-labels for concentrations of the molecules lower than 10% in the solution. The NEXAFS experiments reveal first that the molecules of a pure stearic acid film are tilted by 37° with respect to the surface normal. Owing to the doping of the films with the spin probes, gauche defects are introduced to the structure, but the basic adsorption geometry remains as long as the concentration of the spin-labels is sufficiently low. The temperature-dependent EPR spectra exhibit two major effects. First, the onset for the rotational motion of the spin-label is shifted drastically toward higher temperatures if the distance between the spin-label and surface is reduced from the 16- to the 5- doxyl stearic acid. Second, it is possible to identify a second dynamic mode, namely the rotation of the methylene groups in the neighborhood of the spin-label due to a Gaussian broadening of the spectra.

Acknowledgment. We are grateful to the Deutsche Forschungsgemeinschaft, the Ministerium für Wissenschaft und Forschung des Landes Nordrhein-Westfalen, the Bundesministerium für Bildung und Forschung, and the Fonds der Chemischen Industrie for financial support. We would like to thank Prof. Ch. Wöll for helpful discussions. T.R. wants to thank the Studienstiftung des deutschen Volkes for a fellowship.

References and Notes

(1) Ulman, A. *An Introduction to Ultrathin Organic Films From Langmuir−Blodgett to Self-Assembly*; Academic Press: Boston, 1991.
(2) Lercel, M. J.; Whelan, C. S.; Craighead, H. G.; Seshadri, K. Allara, D. L. *J. Vac. Sci. Technol. B* **1996**, *14*, 4085.
(3) Xia, Y. N.; Zhao, X. M.; Whitesides, G. M. *Microelectron. Eng.* **1996**, *32*, 255.
(4) Spiess, H. W. *Ber. Bunsen-Ges. Phys. Chem.* **1997**, *101*, 153.
(5) Farle, M.; Zomack, M.; Baberschke, K. *Surf. Sci.* **1985**, *160*, 205.
(6) Schlienz, H.; Beckendorf, M.; Katter, U. J.; Risse, T.; Freund, H.-J. *Phys. Rev. Lett.* **1995**, *74*, 761.
(7) Risse, T.; Hill, T.; Beckendorf, M.; Katter, U. J.; Schlienz, H.; Hamann, H.; Freund, H.-J. *Langmuir* **1996**, *12*, 5512.
(8) Allara, D. L.; Nuzzo, R. G. *Langmuir* **1985**, *1*, 45.
(9) Allara, D. L.; Nuzzo, R. G. *Langmuir* **1985**, *1*, 52.
(10) March, D. In *Membrane Spectroscopy*; Grell, E., Ed.; Springer: Berlin, 1981; pp 51−142.
(11) Katter, U. J.; Schlienz, H.; Beckendorf, M.; Freund, H.-J. *Ber. Bunsen-Ges. Phys. Chem.* **1993**, *97*, 340.
(12) Cappus, D. Ph.D. Thesis, Ruhr-Universität Bochum, 1995.
(13) Jaeger, R. M.; Kuhlenbeck, H.; Freund, H.-J.; Wuttig, M.; Hoffmann, W.; Franchy, R.; Ibach, H. *Surf. Sci.* **1991**, *259*, 235.
(14) Risse, T.; Hill, T.; Schmidt, J.; Abend, G.; Hamann, H.; Freund, H.-J. *J. Chem. Phys.*, accepted.
(15) Beckendorf, M. Ph.D. Thesis, Ruhr-Universität Bochum, 1995.
(16) Schneider, D. J.; Freed, J. H. Calculating slow motional magnetic resonance spectra: A user's guide. In *Spin Labeling Theory and Applications*; Berliner, L. J., Reuben, J., Eds.; Plenum Press: New York, 1989; Vol. 8.
(17) Schneider, D. J.; Freed, J. H. Lasers, Spin Relaxation and Motional Dynamics. In *Advances in Chemical Physics*; John Wiley & Sons: New York, 1989; Vol. 73.
(18) Offord, D. A.; John, C. M.; Linford, M. R.; Griffin, J. H. *Langmuir* **1994**, *10*, 883.
(19) Bonosi, F.; Gabrielli, G.; Martini, G.; Ottaviani, M. F. *Langmuir* **1989**, *5*, 1037.
(20) Martini, G.; Bonosi, F.; Ottaviani, M. F.; Gabrielli, G. *Thin Solid Films* **1989**, *178*, 271.

(21) Stöhr, J. NEXAFS Spectroscopy; *Springer Series in Surface Science*; Springer: Berlin, 1992; Vol. 25.
(22) Outka, D. A.; Stöhr, J.; Rabe, J. P.; Swalen, J. D. *J. Chem. Phys.* **1988**, *88*, 4076.
(23) Bagus, P. S.; Weiss, K.; Schertel, A.; Wöll, C.; Braun, W.; Hellwig, C.; Jung, C. *Chem. Phys. Lett.* **1996**, *258*, 129.
(24) Outka, D. A.; Stöhr, J.; Rabe, J. P.; Swalen, J. D.; Rothermund, H. H. *Phys. Rev. Lett.* **1987**, *59*, 1321.
(25) Hähner, G.; Kinzler, M.; Wöll, C.; Grunze, M.; Scheller, M. K.; Cederbaum, L. S. *Phys. Rev. Lett.* **1991**, *67*, 851.
(26) Kinzler, M.; Schertel, A.; Hähner, G.; Wöll, C.; Grunze, M.; Albrecht, H.; Holzhüter, G.; Gerber, T. *J. Chem. Phys.* **1994**, *10*, 7722.
(27) Schertel, A.; Hähner, G.; Grunze, M.; Wöll, C. *J. Vac. Sci. Technol. A* **1996**, *14*, 1801.
(28) Hähner, G.; Kinzler, M.; Thümmler, C.; Wöll, C.; Grunze, M. *J. Vac. Sci. Technol. A* **1992**, *10*, 2758.
(29) Bierbaum, K.; Kinzler, M.; Wöll, C.; Grunze, M.; Hähner, G.; Heid, S.; Effenberger, F. *Langmuir* **1995**, *11*, 512.
(30) Holldack, K.; Grunze, M.; Kinzler, M.; Kerkow, H.; Brundle, C. R. *J. Electron. Spectrosc. Relat. Phenom.* **1995**, *73*, 239.
(31) Hähner, G.; Wöll, C.; Buck, M.; Grunze, M. *Langmuir* **1993**, *9*, 1955.
(32) Somers, J.; Robinson, A. W.; Lindner, T.; Ricken, D.; Bradshaw, A. M. *Phys. Rev. B* **1989**, *40*, 2053.
(33) Tobin, M. C. *J. Mol. Spectrosc.* **1960**, *4*, 349.
(34) Stöhr, J.; Outka, D. A.; Baberschke, K.; Arvanitis, D.; Horsley, J. A. *Phys. Rev. B* **1987**, *36*, 2976.
(35) Ohta, T.; Seki, K.; Yokoymama, T.; Morisada, I.; Edamatsu, K. *Phys. Scr.* **1990**, *41*, 150.
(36) Dubois, L. H.; Zegarski, B. R.; Nuzzo, R. G. *J. Electron. Spectrosc. Relat. Phenom.* **1990**, *54/55*, 1143.
(37) Samant, M. G.; Brown, C. A.; Gordon II, J. G. *Langmuir* **1993**, *9*, 1082.
(38) Thompson, W. R.; Pemberton, J. E. *Langmuir* **1995**, *11*, 1720.
(39) Smith, E. L.; Porter, M. D. *J. Phys. Chem.* **1993**, *97*, 8032.
(40) Libertini, L. J.; Griffith, O. H. *J. Chem. Phys.* **1970**, *53*, 1359.
(41) Nuzzo, R. G.; Dubois, L. H.; Allara, D. L. *J. Am. Chem. Soc.* **1990**, *112*, 558.
(42) Nuzzo, R. G.; Fusco, F. A.; Allara, D. L. *J. Am. Chem. Soc.* **1987**, *109*, 2358.
(43) Katter, U. J. Ph.D. Thesis, Ruhr-Universität Bochum, 1995.
(44) Katter, U. J.; Hill, T.; Risse, T.; Schlienz, H.; Beckendorf, M.; Klüner, T.; Hamann, H.; Freund, H.-J. *J. Phys. Chem. B* **1997**, *101*, 552.
(45) Ge, M.; Freed, J. H. *Biophys. J.* **1993**, *65*, 2106.
(46) Hubbell, W. L.; McConnell, H. M. *J. Am. Chem. Soc.* **1971**, *93*, 314.
(47) Lange, A.; Marsh, D.; Wassmer, K.-H.; Meier, P.; Kothe, G. *Biochemistry* **1985**, *24*, 4383.
(48) Schindler, H.; Seelig, J. *J. Chem. Phys.* **1973**, *59*, 1841.
(49) Michon, P.; Rassat, A. *Bull. Soc. Chim. Fr.* **1971**, *10*, 3561.
(50) Michon, P.; Rassat, A. *J. Org. Chem.* **1974**, *39*, 2121.
(51) Eaton, S. S.; van Willigen, H.; Heinig, M. J.; Eaton, G. R. *J. Magn. Reson.* **1980**, *38*, 325.
(52) Heinig, M. J.; Eaton, G. R.; Eaton, S. S. *Org. Magn. Reson.* **1978**, *11*, 211.
(53) Heinig, M. J.; Eaton, G. R.; Eaton, S. S. *Appl. Spectrosc.* **1980**, *34*, 268.
(54) Schatzki, T. F. *J. Polym. Sci.* **1962**, *57*, 496.
(55) Ferrarini, A.; Nordio, P. L.; Moro, G. J.; Crepeau, R. H.; Freed, J. H. *J. Chem. Phys.* **1989**, *91*, 5707.
(56) Helfand, E.; Skolnick, J. *J. Chem. Phys.* **1982**, *77*, 5714.
(57) Skolnick, J.; Helfand, E. *J. Chem. Phys.* **1980**, *72*, 5489.
(58) Chidsey, C. E. D.; Liu, G.-L.; Rowntree, P.; Scoles, G. *J. Chem. Phys.* **1989**, *91*, 4421.
(59) Gaffney, B. J.; McConnell, H. M. *J. Magn. Reson.* **1974**, *16*, 1.